Mecánica Computacional Vol. XXII
M. B. Rosales, V. H. Cortínez y D. V. Bambill (Editores)
Bahía Blanca, Argentina, Noviembre 2003

CALCULATING NUMERIC DISPERSIVE PROPERTIES OF FEM'S FOR THE 2D AND 3D ELASTIC WAVE EQUATION

Fabio I. Zyserman*and Patricia M. Gauzellino†

*CONICET, Instituto de Física de La Plata,
CC 67, 1900 La Plata, Argentina,
e-mail: zyserman@fcaglp.unlp.edu.ar

†Fac. de Cs. Astronómicas y Geofísicas, UNLP,
Paseo del Bosque s/n, 1900 - La Plata, Argentina.
e-mail: gauze@fcaglp.unlp.edu.ar

Key Words: Finite elements, numerical dispersion, elastic equation.

Abstract. *We investigate the numerical dispersive properties of nonconforming finite element methods to solve the two and three dimensional elastodynamic equations. The study is performed by deriving and analysing the dispersion relations and by evaluating the derived quantities, such as the dimension-less phase and group velocities. Also the phase difference between exact and numerical solutions is investigated. The method studied, which yields a linear spatial approximation, demonstrates to be less dispersive than conforming bilinear finite element methods yielding the same spatial degree of approximation in the two cases shown herein.*

1 INTRODUCTION

Nonconforming finite element methods for the wave equations have been studied by[1,2] and[3] used these numerical procedures to model problems of exploration geophysics.

A review of literature on effects of numerical dispersion in propagation of wave phenomena reveals that most of the articles published on this subject deal with 2-D scalar wave equation[4–8] and 3-D scalar case.[9–11] An exception are the studies by Bamberger et al.[12] and Marfurt[13] which analyse the 2-D elastic wave equation. In order to reduce this gap, our work investigates what can be gained by using a nonconforming finite element method in 2-D and 3-D elastic wave equation computations.

In the following sections we test if this numerical scheme with a strong theoretical background is, at the same time, of practical utility. First the differential equations to elastic wave propagation modeling is provided. Next, the numerical procedure is considered. This is followed by the calculation of the dispersion relations and thorough analysis of its properties. Finally, discussion of results and the concluding remarks are presented.

2 THE ELASTIC WAVE EQUATION

The equations describing elastic wave propagation in a two-dimensional or three-dimensional medium, are: the strain-displacement relation

$$\varepsilon_{ij}(\widehat{u}) = \frac{1}{2}\left(\frac{\partial \widehat{u}_i}{\partial x_j} + \frac{\partial \widehat{u}_j}{\partial x_i}\right), \tag{1}$$

the stress-strain relation

$$\widehat{\tau}_{ij}(\widehat{u}) = \lambda(x)\delta_{ij}\varepsilon_{kk}(\widehat{u}) + 2\mu(x)\varepsilon_{ij}(\widehat{u}), \tag{2}$$

the equation of dynamics

$$-\rho(x)\omega^2\widehat{u}(x,\omega) - \nabla\cdot\widehat{\tau} = \widehat{f}(x,\omega), \quad x\in\Omega=(0,1)^N, N=2,3, \tag{3}$$

and boundary conditions

$$-\widehat{\tau}\nu = i\omega\mathcal{A}\widehat{u}, \quad x\in\Gamma, \tag{4}$$

where $\hat{u}(x,\omega)$ is the Fourier transform of the displacement vector $u(x,t)$ at the real angular frequency ω. In (2), λ and μ are elastic constants. In (3), $\rho(x)$ is the density of the medium and $f(x,t)$ is the external source. The derivation of the absorbing boundary conditions (4) can be found in.[14,15]

For $N=2$

$$\mathcal{A} = \rho(x)\begin{bmatrix} \nu_1 & \nu_2 \\ -\nu_2 & \nu_1 \end{bmatrix}\begin{bmatrix} v_P & 0 \\ 0 & v_S \end{bmatrix}\begin{bmatrix} \nu_1 & -\nu_2 \\ \nu_2 & \nu_1 \end{bmatrix},$$

and for $N=3$,

$$\mathcal{A} = \rho(x)\begin{bmatrix} \nu_1 & \nu_2 & \nu_3 \\ \tau_1^1 & \tau_2^1 & \tau_3^1 \\ \tau_1^2 & \tau_2^2 & \tau_3^2 \end{bmatrix}\begin{bmatrix} v_P & 0 & 0 \\ 0 & v_S & 0 \\ 0 & 0 & v_S \end{bmatrix}\begin{bmatrix} \nu_1 & \tau_1^1 & \tau_1^2 \\ \nu_2 & \tau_2^1 & \tau_2^2 \\ \nu_3 & \tau_3^1 & \tau_3^2 \end{bmatrix}.$$

Here τ_1 and τ_2 are two unit tangent vectors on the boundary Γ such that $\{\nu, \tau_1, \tau_2\}$ is an orthogonal set. The phase velocities of compressional and shear waves are $v_P = \left(\frac{\lambda+2\mu}{\rho}\right)^{\frac{1}{2}}$ and $v_S = \left(\frac{\mu}{\rho}\right)^{\frac{1}{2}}$ respectively.

3 NUMERICAL FORMULATION

The finite element technique, summarized below, for obtaining an approximation solution was introduced and analysed in.[1] Let $H^1(\Omega)$ be the Sobolev space of functions in $L^2(\Omega)$ with first derivatives in $L^2(\Omega)$. The weak form of the problem is found as usual by multiplying the equation (3) by admissible test functions and then integrating by parts. The resulting equation is

$$-(\rho\omega^2\widehat{u}, \psi) + \sum_{pq}(\tau_{pq}(\widehat{u}), \varepsilon_{pq}(\psi)) + i\omega \langle \mathcal{A}\widehat{u}, \varphi\rangle_\Gamma = (\widehat{f}, \psi), \quad \psi \in [H^1(\Omega)]^N. \tag{5}$$

In the above equation $(f, g) = \int_\Omega f\overline{g}\, dx$ and $\langle f, \overline{g}\rangle = \int_\Gamma f\overline{g}\, d\Gamma$ denote the complex $[L^2(\Omega)]^N$ and $[L^2(\Gamma)]^N$ inner products.

The nonconforming Galerkin procedure consists of finding approximatios to $\widehat{u}$. Since the two-dimensional case was also presented in,[16] we are made aware here of the three-dimensional case. We define on the reference cube $\widehat{R} = [-1, 1]^3$

$$S_3(\widehat{R}) = \text{Span}\left\{1, x, y, z, \xi(z) - \xi(x), \xi(z) - \xi(y)\right\}, \quad \xi(x) = x^2 - \frac{5}{3}x^4, \tag{6}$$

The six degrees of freedom associated with $S_3(\widehat{R})$ are the values at the mid points of the faces of $\widehat{R}$. For example, the basis function associated with P=(0,1,0), the E node in Fig.1, is $\varphi_E(x, y, z) = \frac{1}{6} + \frac{1}{2}y + \frac{1}{4}(\xi(x) - 2\xi(y) + \xi(z))$; it takes value one at the P node and zero on the remaining ones. The same happens with the other basis functions and their respective associated nodes. We mention here that the other five basis functions can be obtained by reflection on the three coordinate planes and cyclic permutation of the variables.

Next we formulate the procedure as follows: find $\widehat{u}^h \in [NC^h]^N$ such that

$$-(\rho\omega^2\widehat{u}^h, \psi) + \sum_{pq}(\tau_{pq}(\widehat{u}^h), \varepsilon_{pq}(\psi)) + i\omega \left\langle\!\!\left\langle \mathcal{A}\widehat{u}^h, \varphi\right\rangle\!\!\right\rangle_\Gamma = (\widehat{f}, \psi), \quad \psi \in [MC^h]^N. \tag{7}$$

where $\langle\!\langle ., .\rangle\!\rangle$ is the notation for computing the boundary using the midpoint quadrature rule.

4 DISPERSION ANALYSIS

4.1 Dispersion Relations

To perform the dispersion analysis, we must obtain the basic algebraic equation of a typical degree of freedom.[12,13] In equation (7), we set the source term to zero and restrict

ourselves to a portion of the domain far away from the boundaries so we can ignore their contribution.

Fig.(1) shows stencils of elements and nodes involved in the correct building of a structure using these nodes. Since the origin of coordinates is not a node of the nonconforming grid, it was necessary to consider a global test function φ_G.

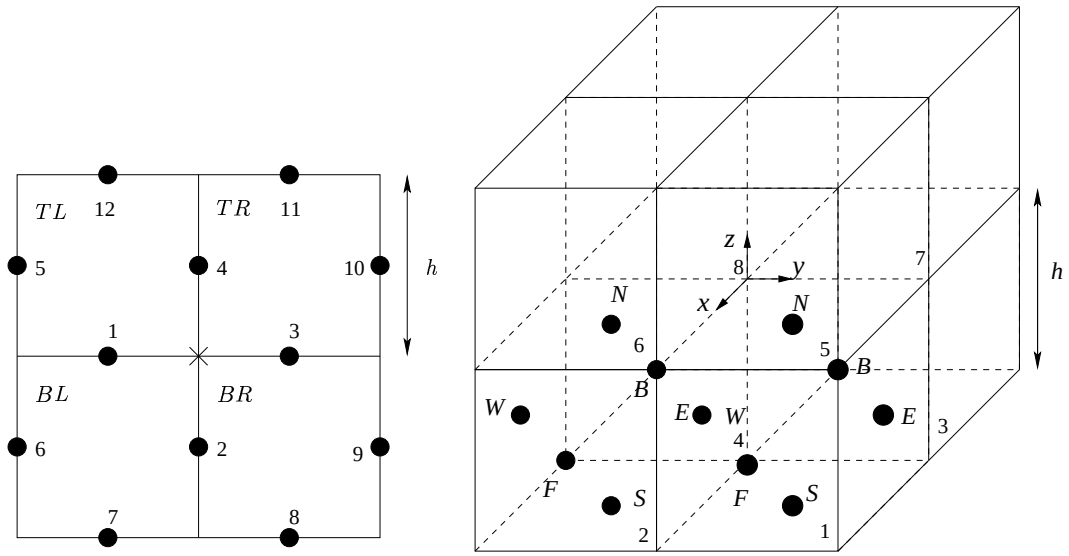

Figure 1: *Elements and nodes involved in the calculation of the numeric dispersion relations for (a) 2-D case and (b) 3-D case.*

For $N = 2$

$$\varphi_G = \begin{cases} \psi_b & \text{on node 1} \quad \text{in } TL \\ \psi_t & \text{on node 1} \quad \text{in } BL \\ \psi_r & \text{on node 2} \quad \text{in } BL \\ \psi_l & \text{on node 2} \quad \text{in } BR \\ \psi_b & \text{on node 3} \quad \text{in } TR \\ \psi_t & \text{on node 3} \quad \text{in } BR \\ \psi_r & \text{on node 4} \quad \text{in } TL \\ \psi_l & \text{on node 4} \quad \text{in } TR, \end{cases} \tag{8}$$

and for $N = 3$

$$\varphi_G = \begin{cases} \varphi_W(x,y,z) + \varphi_B(x,y,z) + \varphi_N(x,y,z) & \text{in} \quad \Omega_1 \\ \varphi_E(x,y,z) + \varphi_B(x,y,z) + \varphi_N(x,y,z) & \text{in} \quad \Omega_2 \\ \varphi_W(x,y,z) + \varphi_F(x,y,z) + \varphi_N(x,y,z) & \text{in} \quad \Omega_3 \\ \varphi_E(x,y,z) + \varphi_F(x,y,z) + \varphi_N(x,y,z) & \text{in} \quad \Omega_4 \\ \varphi_W(x,y,z) + \varphi_B(x,y,z) + \varphi_S(x,y,z) & \text{in} \quad \Omega_5 \\ \varphi_E(x,y,z) + \varphi_B(x,y,z) + \varphi_S(x,y,z) & \text{in} \quad \Omega_6 \\ \varphi_W(x,y,z) + \varphi_F(x,y,z) + \varphi_S(x,y,z) & \text{in} \quad \Omega_7 \\ \varphi_E(x,y,z) + \varphi_F(x,y,z) + \varphi_S(x,y,z) & \text{in} \quad \Omega_8 \end{cases} \tag{9}$$

φ_G are piecewise functions, where each piece is a local basis function, contributing only when its support, the corresponding domain, is considered in the calculation of the internal products of equation (7). For example, in the two-dimensional case, we replace the vector test function by (φ_G, φ_G) and consider $\widehat{u} = (v, w)$ as a superposition of the product of the unknown coefficients v_i, $i = 1, \ldots, 12$ and w_j, $j = 1, \ldots, 12$ times the associated basis functions; i.e.,

$$\begin{aligned} -\rho h^2 \left(\frac{35}{84}(v_1 + v_2 + v_3 + v_4) + \frac{1}{24}(v_5 + v_6 + v_7 + v_8 + v_9 + v_{10} + v_{11} + v_{12}) \right) \\ + \mu \left(2(v_1 + v_3) - (v_7 + v_8 + v_{11} + u_{12})\right) \\ + (\lambda + 2\mu) \left(2(v_2 + v_4) - (v_5 + v_6 + v_9 + v_{10})\right) \\ + \mu(w_5 + w_9 - w_6 - w_{10}) + \lambda(w_8 + w_{12} - w_7 - w_{11}) = 0 \end{aligned}$$

$$\begin{aligned} -\rho h^2 \left(\frac{35}{84}(w_1 + w_2 + w_3 + w_4) + \frac{1}{24}(w_5 + w_6 + w_7 + w_8 + w_9 + w_{10} + w_{11} + w_{12}) \right) \\ + \mu \left(2(w_2 + w_4) - (v_5 + v_6 + v_9 + u_{10})\right) \\ + (\lambda + 2\mu) \left(2(w_1 + w_3) - (w_7 + w_8 + w_{11} + v_{12})\right) \\ + \lambda(u_5 + u_9 - u_6 - u_{10}) + \mu(u_8 + u_{12} - u_7 - u_{11}) = 0. \end{aligned} \tag{10}$$

Following Bamberger et al.,[12] we assume wave fields of the form $(d_1, d_2) \exp(\pm i \mathbf{k}^h \mathbf{x})$ with origin in the x-marked node, angular frequency ω and obtain

$$-\rho\omega^2 h^2 T \begin{pmatrix} d_1 \\ d_2 \end{pmatrix} + \mathbf{B} \begin{pmatrix} d_1 \\ d_2 \end{pmatrix} = 0, \tag{11}$$

where T is

$$T = \frac{1}{12} \left(5 \left(\cos(\tfrac{1}{2}k_1^h h) + \cos(\tfrac{1}{2}k_2^h h)\right) + \cos(k_1^h h)\cos(\tfrac{1}{2}k_2^h h) + \cos(\tfrac{1}{2}k_1^h h)\cos(k_2^h h)\right). \tag{12}$$

and $\mathbf{B}$ is the dispersion matrix with elements

$$
\begin{aligned}
b_{11} &= 2\mu\cos(\tfrac{1}{2}k_1^h h)(1-\cos(k_2^h h)) + 2(\lambda+2\mu)\cos(\tfrac{1}{2}k_2^h h)(1-\cos(k_1^h h)) \\
b_{12} &= 2\mu\sin(k_1^h h)\sin(\tfrac{1}{2}k_2^h h) + 2\lambda\sin(\tfrac{1}{2}k_1^h h)\sin(k_2^h h) \\
b_{21} &= 2\lambda\sin(k_1^h h)\sin(\tfrac{1}{2}k_2^h h) + 2\mu\sin(\tfrac{1}{2}k_1^h h)\sin(k_2^h h) \\
b_{22} &= 2\mu\cos(\tfrac{1}{2}k_2^h h)(1-\cos(k_1^h h)) + 2(\lambda+2\mu)\cos(\tfrac{1}{2}k_1^h h)(1-\cos(k_2^h h))
\end{aligned} \tag{13}
$$

Equation (11) implies that $\rho\omega^2 h^2 T$ is an eigenvalue of $\mathbf{B}$ with an associated eigenvector given by (d_1, d_2). For any fixed k, this equation determines two solutions,

$$
\omega_j = \sqrt{\frac{\Lambda_j}{\rho h^2 T}}, \quad j = 1, 2, \tag{14}
$$

yielding the numeric dispersion relation, where Λ_j, $j = 1, 2$ are the eigenvalues of the matrix $\mathbf{B}$.

Proceeding in analogy to the previous case, in 3-D, we obtain an expresion similar to (10), which we will omit considering that the test function are $(\varphi_G, \varphi_G, \varphi_G)$ and $\widehat{u} = (v, w, z)$ which now 36 unknown coefficients per component.

Afterwards we replace the unknowns by the corresponding plane wave solution and we obtain the following system of three equations

$$
-\rho\omega^2 h^2 T \begin{pmatrix} d_1 \\ d_2 \\ d_3 \end{pmatrix} + \mathbf{B} \begin{pmatrix} d_1 \\ d_2 \\ d_3 \end{pmatrix} = 0, \tag{15}
$$

$\mathbf{B}$ being the dispersion matrix with elements given by

$$
\begin{aligned}
b_{11} &= \mu\,\gamma_1(\beta_2^2\,\gamma_3 + \beta_3^2\,\gamma_2) + (\lambda+2\,\mu)\,\beta_1^2\,\gamma_2\,\gamma_3, \\
b_{12} &= \beta_1\,\beta_2\,\gamma_3\,(\mu\,\gamma_1 + \lambda\,\gamma_2)\,, \\
b_{13} &= \beta_1\,\beta_3\,\gamma_2\,\,(\mu\,\gamma_1 + \lambda\,\gamma_3)\,, \\
b_{21} &= \beta_1\,\beta_2\,\gamma_3\,(\lambda\,\gamma_1 + \mu\,\gamma_2)\,, \\
b_{22} &= \mu\,\gamma_2(\beta_3^2\,\gamma_1 + \beta_1^2\,\gamma_3) + (\lambda+2\,\mu)\,\beta_2^2\,\gamma_1\,\gamma_3, \\
b_{23} &= \beta_2\,\beta_3\,\gamma_1(\mu\,\gamma_2 + \lambda\,\gamma_3), \\
b_{31} &= \beta_1\,\beta_3\,\gamma_2(\lambda\,\gamma_1 + \mu\,\gamma_3), \\
b_{32} &= \beta_2\,\beta_3\,\gamma_1(\lambda\,\gamma_2 + \mu\,\gamma_3), \\
b_{33} &= \mu\,\gamma_3(\beta_2^2\,\gamma_1 + \beta_1^2\,\gamma_2) + (\lambda+2\,\mu)\,\beta_3^2\,\gamma_1\,\gamma_2.
\end{aligned} \tag{16}
$$

with

$$
\begin{aligned}
&\gamma_1 = \cos(\tfrac{1}{2}k_1^h h), \quad \gamma_2 = \cos(\tfrac{1}{2}k_2^h h), \quad \gamma_3 = \cos(\tfrac{1}{2}k_3^h h), \\
&\beta_1 = \sin(\tfrac{1}{2}k_1^h h), \quad \beta_2 = \sin(\tfrac{1}{2}k_2^h h), \quad \beta_3 = \sin(\tfrac{1}{2}k_3^h h).
\end{aligned} \tag{17}
$$

Given k, this system determines the solutions

$$\omega_j(k^h) = \sqrt{\frac{\Lambda_j}{\rho h^2 T}}, \quad j = 1, 2, 3, \tag{18}$$

where Λ_j, $j = 1, 2, 3$ are the eigenvalues of the dispersion matrix.

4.2 Dispersion Properties

Grid coarseness is an important parameter that affects the accuracy of numerical methods. The number of grid points per wavelength of a plane wave of frequency ω is a measure of grid coarseness. We will use H, the reciprocal of the number of grid points per wavelength and write $k^h = (k_1^h, k_2^h, k_3^h) = 2\pi H(\cos\theta, \sin\theta)$ and $k^h = (k_1^h, k_2^h, k_3^h) = 2\pi H(\cos\theta\cos\phi, \sin\theta\cos\phi, \sin\phi)$; recalling that $|k| = \frac{2\pi}{\lambda}$ and being θ the angle between the direction of propagation and the x-axis and ϕ the angle between k and the z-axis. Let us make the nodal separation in the mesh $h \to 0$ for any fixed k. We develop the elements of matrix $\mathbf{B}$ and T in terms of h.

For $N = 2$

$$\begin{aligned}
b_{11} &\simeq \left(k_2^2\,\mu + k_1^2\,(\lambda + 2\,\mu)\right)\, h^2 + O(h)^4,\\
b_{12} &\simeq k_1\,k_2\,(\lambda + \mu)\, h^2 + O(h)^4,\\
b_{21} &\simeq k_1\,k_2\,(\lambda + \mu)\, h^2 + O(h)^4,\\
b_{22} &\simeq \left(k_1^2\,\mu + k_2^2\,(\lambda + 2\,\mu)\right)\, h^2 + O(h)^4.
\end{aligned} \tag{19}$$

Furthermore,

$$T \simeq 1 - \frac{5}{48}\left(k_1^2 + k_2^2\right) h^2 + O(h)^4, \tag{20}$$

corresponding to compressional and shear waves, respectively. The two eigenvalues are

$$\Lambda_1 \simeq h^2(\lambda + 2\,\mu)\,\left(k_1^2 + k_2^2\right) + O(h)^4 \quad \Lambda_2 \simeq h^2\mu\,\left(k_1^2 + k_2^2\right) + O(h)^4. \tag{21}$$

The phase and group velocities of the two solutions are

$$\frac{\omega_1}{|k|} \simeq \sqrt{\frac{\lambda + 2\,\mu}{\rho}} + O(h)^2 \text{ and } \frac{\omega_2}{|k|} \simeq \sqrt{\frac{\mu}{\rho}} + O(h)^2 \tag{22}$$

and

$$Q_P = \nabla\omega_1 \frac{k}{|k|}, \quad Q_S = \nabla\omega_2 \frac{k}{|k|}, \tag{23}$$

We can prove in[16] that an infinite elastic medium with no damping is nondispersive.

For $N = 3$ In like manner, expanding the elements of matrix $\mathbf{B}$ and T in terms of h one obtains

$$\mathbf{B} \simeq 4h^2\tilde{\mathbf{B}} + O(h^3) \tag{24}$$

where $\tilde{\mathbf{B}}$ is a symmetric matrix with elements

$$\begin{aligned}
\tilde{b}_{11} &= \mu\,(k_2^2 + k_3^2) + (\lambda + 2\mu)\,k_1^2,\\
\tilde{b}_{12} &= (\lambda + \mu)\,k_1\,k_2,\\
\tilde{b}_{13} &= (\lambda + \mu)\,k_1\,k_2,\\
\tilde{b}_{22} &= \mu\,(k_1^2 + k_3^2) + (\lambda + 2\mu)\,k_2^2,\\
\tilde{b}_{23} &= (\lambda + \mu)\,k_2\,k_3,\\
\tilde{b}_{33} &= \mu\,(k_1^2 + k_2^2) + (\lambda + 2\mu)\,k_3^2
\end{aligned} \tag{25}$$

and

$$T \simeq 4 - \frac{1}{3}|k^h|^2 h^2 + O(h)^3. \tag{26}$$

The three eigenvalues of $\mathbf{B}$ can be casted as

$$\begin{aligned}
\Lambda_1 &\simeq h^2(\lambda + 2\,\mu)\,|k^h|^2 + O(h)^3,\\
\Lambda_2 &\simeq h^2\mu\,|k^h|^2 + O(h)^3,\\
\Lambda_3 &\simeq h^2\mu\,|k^h|^2 + O(h)^3.
\end{aligned} \tag{27}$$

The corresponding expressions for phase and group velocities is obtained by replacing in Eq. (18)

$$\frac{\omega_1}{|k^h|} \simeq \sqrt{\frac{\lambda + 2\,\mu}{\rho}} + O(h) \text{ and } \frac{\omega_{2,3}}{|k^h|} \simeq \sqrt{\frac{\mu}{\rho}} + O(h). \tag{28}$$

$$Q_P = \nabla\omega_1 \frac{k^h}{|k^h|}, \quad Q_S = \nabla\omega_2 \frac{k^h}{|k^h|}, \tag{29}$$

We recover the velocities of compressional and shear waves for small values of h. We must prove that ω_j, $j = 1, 2, 3$ are real because we have assumed a model without dissipation. Therefore, the eigenvalues in Eq. (18) must in turn be real, a condition that unfortunately they do not automatically verify, because the dispersion matrix $\mathbf{B}$ is in general not symmetric, as shown by Eq. (16). Let us write down the eigenvalues explicitly:

$$\Lambda_1 = W + Z, \qquad \Lambda_2 = W - Z, \qquad \Lambda_3 = X, \tag{30}$$

where

$$X = 16\mu\left(\gamma_2\gamma_3\,\beta_1^2 + \gamma_1\gamma_3\,\beta_2^2 + \gamma_1\gamma_2\beta_3^2\right),$$
$$W = 8\left(\lambda + 3\,\mu\right)\left(\gamma_2\gamma_3\beta_1^2 + \gamma_1\gamma_3\beta_2^2 + \gamma_1\gamma_2\beta_3^2\right),$$
$$Z = 8\sqrt{\lambda^2\left(\gamma_2\gamma_3\beta_1^2 + \gamma_1\gamma_3\beta_2^2 + \gamma_1\gamma_2\beta_3^2\right)^2 + \mu^2\left(\gamma_1^2\gamma_3^2\beta_2^4 + \gamma_2^2(\gamma_3\beta_1^2 + \gamma_1\beta_3^2)^2\right)}$$
$$\overline{+\mu^2\left(2\gamma_1\gamma_2\gamma_3\beta_2^2(4(\gamma_1^2\gamma_3 + \gamma_1\gamma_3^2) + 5(\gamma_3\beta_1^2 + \gamma_1\beta_3^2)) - 8\gamma_1\gamma_2\gamma_3\beta_2^2(\gamma_1 + \gamma_3)\right)}$$
$$\overline{+2\lambda\mu(\gamma_2^2\gamma_3^2\beta_1^4 + 4\gamma_1^2\gamma_2\gamma_3^2\beta_2^2(\gamma_1 + \gamma_3) + 2\gamma_3^2\beta_1^2\beta_2^2(\gamma_1^2 + \gamma_1\gamma_2 + \gamma_2^2) + \gamma_1^2\gamma_3^2\beta_2^4)}$$
$$\overline{+2\lambda\mu(2\gamma_2^2\beta_1^2\beta_3^2(\gamma_1^2 + g_2^2) + \gamma_1^2\beta_2^2\beta_3^2(2 + (\gamma_2 + \gamma_3)^2) + \gamma_1^2\gamma_2^2\beta_3^4)}$$
$$\overline{-2\lambda\mu((4\gamma_1\gamma_2\gamma_3\beta_2^2(\gamma_1 + \gamma_3)) + 2\gamma_1\gamma_2^2\gamma_3\beta_1^2\beta_3^2 + \gamma_1^2\beta_2^4\beta_3^2 + \gamma_1^2\beta_2^2\beta_3^4)} \quad (31)$$

The eigenvalues are periodic functions of k, with periodicity equal to $\frac{4\pi}{h}$ and symmetric with respect to the planes $k_1 = 0$, $k_2 = 0$ and $k_3 = 0$. Furthermore, the planes $k_2 = k_1$ and $k_3 = k_1$ are also symmetry planes as the scalar dispersion relation,[16] hence, their domain is $D = \left\{k \in D/|k| \leq \frac{\pi}{h}\right\}$ and $D = \left\{k/0 \leq H \leq \frac{1}{2},\ 0 \leq \theta \leq \frac{\pi}{4},\ 0 \leq \phi \leq \frac{\pi}{4}\right\}$. T being always positive, the eigenvalues must have the same behaviour. Clearly Λ_3 and W are positive, but showing that Z is real and positive is not so obvious. A close inspection shows that the positive terms in Z are always bigger than the negative ones, so it must be shown that $W > Z$. We performed a numerical study of the inequality writing k in terms of H,θ and ϕ, and we found that it is always verified within the prescribed domain, and for all the used Lamé coefficients. For $H \to 0$, $W \simeq 2|k^h|^2(\lambda + 3\mu)$ and $Z \simeq 2|k^h|^2(\lambda + \mu)$, and the eigenvalues recover the continuous behaviour. All eigenvalues remain real and positive also for $H \to \frac{1}{2}$. However, when the number of points per wavelength is smaller than three, although Λ_j, $j = 1, 2, 3$ are positive, the values of the smaller eigenvalues, associated with the S-waves, differ by a small percentage. Nevertheless, this gap diminishes when calculating the dispersion relations and related quantities because one takes the square root of the eigenvalues and divides them by a number bigger than one.

5 RESULTS

To carry on with our task of analysing the numerical error introduced by dispersion, we calculate the dimensionless phase velocities for both P and S waves, since an algorithm may be considered accurate if it properly models these velocities.

The following figures are performed in terms of H, θ, ϕ and the Poisson's coefficient $\nu = \frac{\lambda}{2(\lambda+\mu)}$. Our numerical studies proved that neither the dimensionless phase velocities nor the group velocities depend on the value of Poisson's coefficient, and that they show certain variation only when the number of point per wavelength is smaller than four. This is a very interesting feature, because it makes the numerical method almost independent of the material properties. The restriction of three or four points per wavelength is not a strong one at all, the requirement of having smaller errors in the calculated quantities (exploration geophysicists say 1 percent) usually leads to use at least twice this quantity.

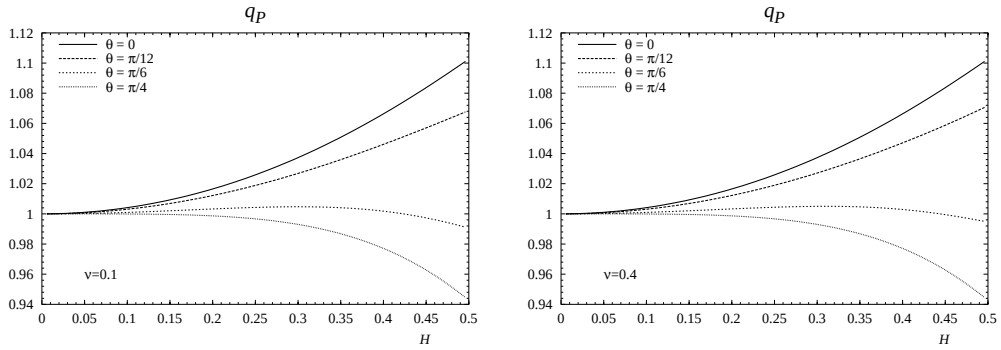

Figure 2: *Adimensional compressional wave phase velocities for two different values of the Poisson's coefficient,* $\nu = 0.1$ *and* $\nu = 0.4$.

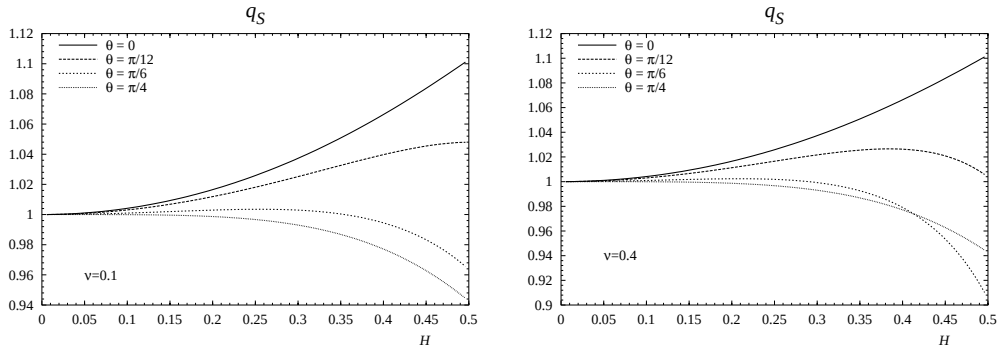

Figure 3: *Adimensional shear wave phase velocities for two different values of the Poisson's coefficient,* $\nu = 0.1$ *and* $\nu = 0.4$.

See Fig.2 and 3 for 2-D case. In the other case, there is almost no variation in the curves when the azimuth θ varies from 0 to $\frac{\pi}{4}$. Then, in order not to show redundant information, we present just one direction. The figure 4 displays compressional and shear phase velocities, calculated for different directions within the prescribed domain and Poisson's coefficient equal 0.1. Fig.5 and 6 show again the dependence of the group velocities on the Poisson's coefficient for 2-D propagation. As before, this dependence is negligible. Adimensional group velocities in 3-D elastic case are illustrated in Fig.7. The horizontal line encloses the region with a relative error of less than 2%. It can be clearly seen that the curves fall inside this region even when calculated with less that ten points per wavelength. Finally we show in Fig.8 and Fig.9 the comparison between the results yielded by the nonconforming method (NC) and the conforming method (C) for the normalized 2-D compressional and shear phase and group velocities. The NC-method is by far less dispersive than the C-one. There is not a big difference in the overall behaviour of the velocities for compressional or shear waves in the case of the former, while for the latter, the shear case display a worse behaviour than the compressional one. When working with ten

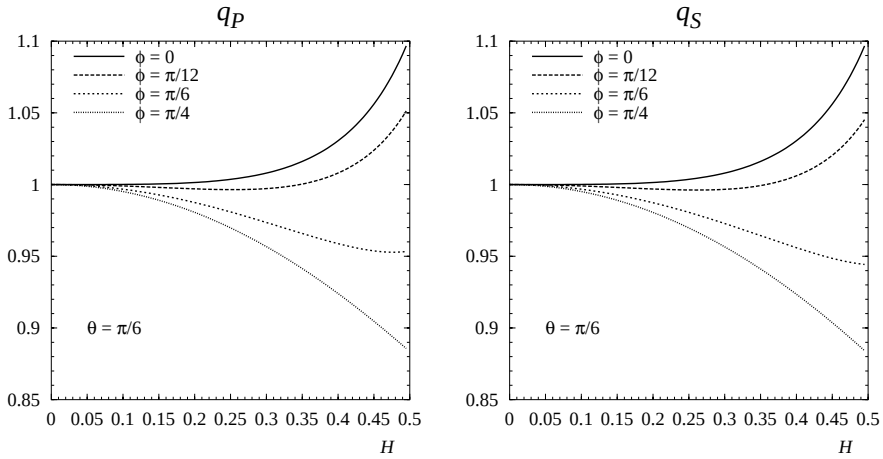

Figure 4: *Adimensional compressional and shear phase velocities for the three dimensional case. Poisson's coefficient,* $\nu = 0.1$.

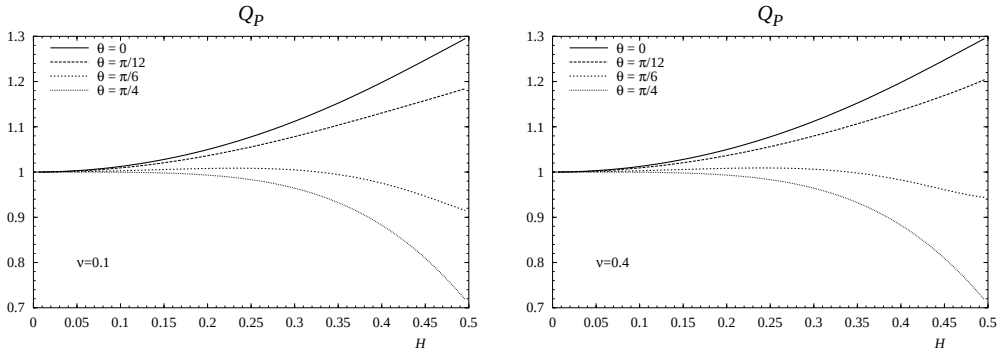

Figure 5: *Adimensional compressional group velocities for two different values of the Poisson's coefficient,* $\nu = 0.1$ *and* $\nu = 0.4$.

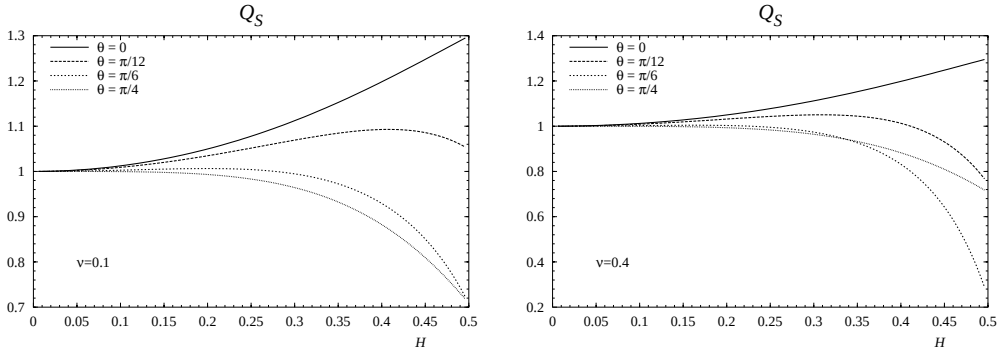

Figure 6: *Adimensional shear wave group velocities for two different values of the Poisson's coefficient,* $\nu = 0.1$ *and* $\nu = 0.4$.

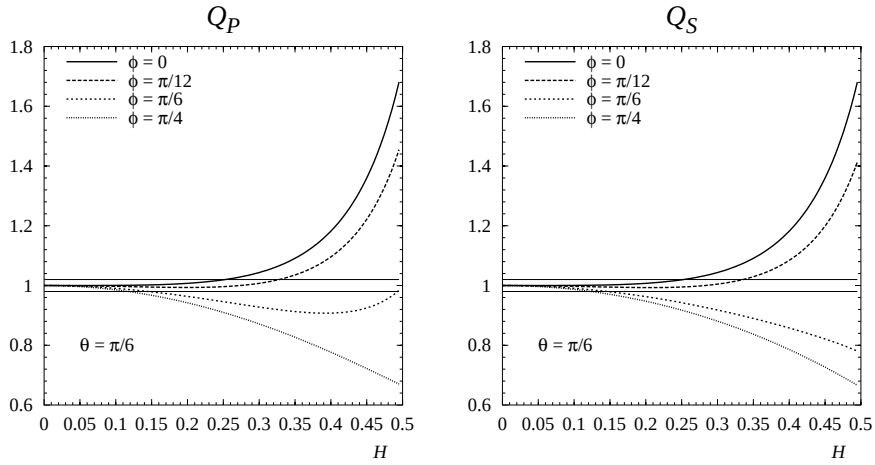

Figure 7: *Adimensional compressional and shear group velocities for the 3-D case. The horizontal lines enclose the region with relative error less than 2%.*

points per wavelength, the error is 5% for the C-method, and .98% for the NC-method, considering the worst case scenarios.

6 CONCLUSIONS

In this paper we have investigated the dispersive properties of a nonconforming finite element method to solve the two-dimensional and three-dimensional elastic wave equations. The study was performed by deriving and analyzing the dispersion relations and by evaluating derived quantities, such as dimensionless phase and group velocities. By means of Taylor expansions of the numerical dispersion relations we showed that the continuous behaviour is recovered, when the distance between nodes tends to be zero simultaneously in all three coordinate directions. We have also observed that the dimensionless phase and group velocities are independent of the material properties of the medium whenever more than three points per wavelength are used.

On the other hand, we have shown that the numerical method introduces spatial anisotropy. The phase and group velocities depend on the propagation directions; however, although they were dependent on the declination ϕ, they presented a small variation for all the ranges of the azimuth. In both cases the phase velocities behave very well, even when using a relatively small number of points per wavelength, the relative error remains close to zero. When dealing with group velocities the number of points per wavelength must be increased to keep this error within small bounds, but we observed that it is possible to have $H > .1$, and the error is still smaller than 2%.

We have studied the (local) phase difference and also observed that the NC-method is polluted, that is, the error of the numerical solution increases for increasing wavenumber, even using a fixed number of points per wavelength.

We have compared the performace of the analyzed method with that of a conforming

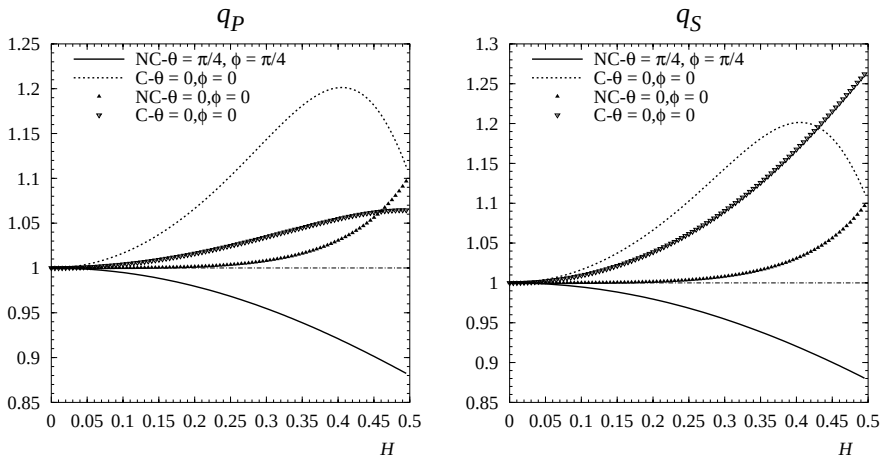

Figure 8: *Comparison of worst (lines) and best (triangles) cases of the compressional and shear phase velocities for the 2-D elastic equation.*

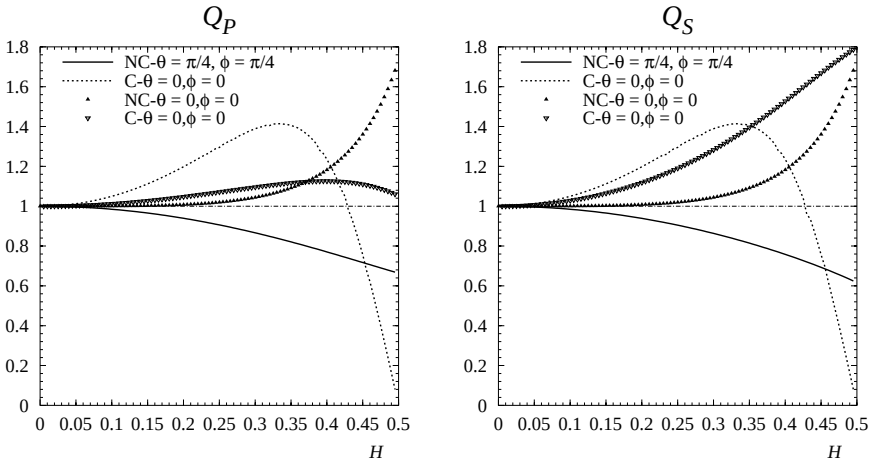

Figure 9: *Comparison of worst (lines) and best (triangles) cases of the compressional and shear group velocities for the 2-D elastic equation.*

finite element method yielding the same order of spatial approximation. It can be clearly seen that the NC-method introduces less numerical anisotropy and is less dispersive than the C-method. Indeed, given a fixed accuracy requirement, using the former allows to nearly halve the number of points per wavelength required by the latter to achieve it.

REFERENCES

[1] J. Douglas, Jr., J. Santos, D. Sheen, and X. Ye. *Mathematical Modelling and Numerical Analysis*, **33**, 744 (1999).

[2] J. Douglas, Jr., J. Santos, and D. Sheen. Nonconforming Galerkin methods for the Hemholtz equation. *Numerical Methods for Partial Differential Equations*, **17**, 475–494 (2001).

[3] P. Gauzellino, J. Santos, and D. Sheen. Frequency domain wave propagation modeling in exploration seismology. *Journal of Computational Acoustics*, **9**(3), 941–955 (2001).

[4] A. Bayliss, C. Goldstein, and E. Turkel. On accuracy conditions for the numerical computation of waves. *J. Comp. Phys.*, **59**, 396–404 (1985).

[5] F. Ihlemburg and I. Babuška. Dispersion analysis and error estimation of Galerkin finite element methods for the Helmholz equation. *Intl. J. for Numerical Methods in Engineering*, **38**, 3745–3774 (1995).

[6] F. Ihlemburg and I. Babuška. Finite element solution of the helmholtz equation with high wave number Part I: the h-version of the FEM. *Computers Math. Applic.*, **30**(9), 9–37 (1995).

[7] F. Ihlemburg and I. Babuška. Finite element solution of the helmholtz equation with high wave number Part II: the $h-p$-version of the FEM. *SIAM J. Numer. Anal.*, **34**(1), 325–358 (1997).

[8] F. Ihlemburg and I. Babuška. Reliability of finite element methods for the numerical computation of waves. *Advances in Engineering Software*, **28**(7), 417–424 (1997).

[9] N.N. Abboud and P.M. Pinsky. *Int. J. Numer. Methods Eng.*, **35**, 1183 (1992).

[10] A. Oberai and P. Pinsky. A residual-based finit element method for the helmholtz equation. *Int. J. Num. Meth. Engineering*, **49**, 399–419 (2000).

[11] H. Kudo, T. Kashiwa, and T. Othani. The nonstandard FDTD method for three-dimensonal acoustic analysis and its numerical dispersion and stability condition. *Electronics and Communications in Japan*, **85**(9), 736 (2002).

[12] A. Bamberger, G. Chavent, and P. Lailly. Etude de schémas numériques pour les équations de l élastodynamique linéaire. Technical Report 41, INRIA, (1980).

[13] K.J. Marfurt. Accuracy of finite-difference and finite-element modelling of the scalar and elastic wave equations. *Geophysics*, **49**, 533 (1984).

[14] C. L. Ravazzoli, J. Douglas, Jr., J. E. Santos, and D. Sheen. On the solution of the equations of motion for nearly elastic solids in the frequency domain. In *Anales de la IV Reunión de Trabajo en Procesamiento de la Información y Control, RPIC'91*, (1991).

[15] D. Sheen, J. Douglas, Jr., and J. E. Santos. Frequency-domain parallel algorithms for the approximation of acoustic and elastic waves. In *Numerical Analysis (Finite Element Methods)*, pages 243–288, (1993).

[16] F. Zyserman, P. Gauzellino, and J. Santos. Dispersion analysis of a non-conforming finite element method for the Helmholtz and elastodynamic equations. *Int. J. Num. Meth. Engineering, in press. Manuscript available from http://sobolev.fcaglp.unlp.edu.ar/˜zyserman/2dd.ps.gz*, (2003).